Sādhanā Vol. 41, No. 6, June 2016, pp. 653–666
DOI 10.1007/s12046-016-0497-4

Analysis of slip flow heat transfer between two unsymmetrically heated parallel plates with viscous dissipation

HARI MOHAN KUSHWAHA* and SANTOSH K SAHU

Discipline of Mechanical Engineering, School of Engineering, Indian Institute of Technology Indore, Indore 453446, India
e-mail: hmkushwaha@gmail.com

MS received 10 March 2015; revised 20 November 2015; accepted 6 January 2016

Abstract. This paper presents an analytical investigation to study the heat transfer and fluid flow characteristics in the slip flow region for hydrodynamically and thermally fully developed flow between parallel plates. Both upper and lower plates are subjected to asymmetric heat flux boundary conditions. The effect of first order velocity slip, temperature jump, asymmetric heat flux ratio and viscous dissipation on the heat transfer performance is analyzed. Closed form expressions are obtained for the temperature distribution and Nusselt number. Present predictions are verified for the cases that neglect the viscous heating and microscale effects. The effect of asymmetric heat flux ratio with and without viscous dissipation on Nusselt number for both macroscale and microscale is highlighted. The heat transfer characteristics are found to depend on various modeling parameters, namely, modified Brinkman number, Knudsen number and heat flux ratio.

Keywords. Knudsen number; modified Brinkman number; temperature jump; velocity slip; viscous dissipation.

1. Introduction

Recent advances in micro technologies and miniaturization of electronics require new approaches to handle higher heat fluxes. For a given volume a microdevice such as micro heat exchanger provides larger heat transfer areas compared to the conventional heat exchanger. In addition, the application of micro technologies is observed in various fields of engineering including micro-electro-mechanical systems (MEMS), microchannel heat sinks for electronic cooling and biomedical engineering [1].

It may be noted that at microscale, the molecular mean free path can be of the same order as the channel diameter. In the case of gaseous flows, the effect of rarefaction is described by the Knudsen number (Kn) and it is defined as the ratio of mean free path (λ) to the characteristic dimension (D_h) of the system. Different flow regimes are classified based on the value of Knudsen number [2]. This includes continuum flow ($Kn < 0.001$), slip flow ($0.001 < Kn < 0.1$), transition flow ($0.1 < Kn < 10$) and free molecular flow ($Kn > 10$). The interaction of fluid with solid surface and the heat transfer in microdevice is different compared to the macrodevice. A gaseous flow in microdevices does not obey the classical continuum physics. On the contrary, the flow exhibits non-zero flow velocity (slip velocity) at the solid wall and the fluid temperature and the solid wall temperature does not remain same at the solid boundaries. This indicates that slip velocity and temperature jump is present at the solid boundaries and found to change the fluid flow and heat transfer characteristics during flow.

Numerous studies have been reported that consider either theoretical simulation or experimental investigation to analyze the flow and heat transfer characteristics of microdevices. These studies considered various factors namely, rarefaction, viscous dissipation, compressibility, axial conduction in their analysis. In addition to the Navier–Stokes and energy equations, these studies used the velocity slip and temperature jump boundary conditions to analyze the flow phenomena [1–4].

The effect of viscous heating is usually considered when the viscosity of the fluid is large or the flow velocity is high. The viscous dissipation effect is usually characterized by the Brinkman number. In the case of microdevices with gaseous flows, even though the velocity is small, the viscous dissipation effect is significant. The role of the viscous dissipation on heat transfer during the flow through microchannels has been studied both through theoretical simulation and experimental investigation [5]. The laminar forced convection in a pipe with viscous dissipation for two different cases such as constant wall temperature and constant heat flux was reported by Aydin [6–9]. It is reported that both aspect ratio of the microchannel and the Reynolds number play an important role in determining the

*For correspondence

influence of the viscous dissipation on the Nusselt number [10]. It is observed that with viscous heating the friction factor decreases with the increase in the Reynolds number [11]. The effects of viscous dissipation and temperature dependent viscosity both in thermally developing and hydrodynamically fully developed flows through the straight microchannels of arbitrary but constant cross-sections were studied by Giudice [12]. The effect of viscous dissipation on the temperature profile and friction factor was studied by Koo and Kleinstreuer [13]. The viscous effects are found to be important for fluids that possess low specific capacities and higher viscosities even with lower Reynolds number flows. Hossainpour and Khadem [14] analyzed the fluid flow and heat transfer in microchannels by applying slip and temperature jump boundary conditions. It is observed that the Nusselt number is more sensitive to the roughness density compared to the roughness shape. Inman [15] studied the heat transfer characteristics of gaseous flows through parallel plates and round tube. The forced convective heat transfer in straight microchannels of uniform but arbitrary cross sections was reported by Hooman [16] employing the superposition approach. Rij *et al* [17] reported the effect of various parameters such as rarefaction and viscous dissipation on Nusselt number. These parameters are found to affect the convective heat transfer rate significantly in the slip flow regime. Tunc and Bayazitoglu [18] reported the convective heat transfer for steady state, laminar, hydrodynamically fully developed flow in microtubes with uniform heat flux boundary conditions by employing integral transform technique. Recently, Kushwaha and Sahu [19, 20] presented closed form solutions for the Nusselt number by using second order velocity slip and temperature jump conditions with viscous dissipation. Miyamoto *et al* [21] reported the effect of viscous dissipation on heat transfer characteristics of choked gas flows through a narrow parallel plate channel by employing uniform heat flux at the walls. The convective heat transfer of the argon gas flow through a micro/nano channel with uniform heat flux wall boundary condition by using the direct simulation Monte Carlo (DSMC) method was reported by Balaj *et al* [22]. In another study the authors [23] considered the effect of shear work due to the velocity slip on the non-equilibrium heat transfer in a pressure driven micro/nano channel under the constant wall heat flux boundary conditions. The effects of rarefaction, property variation and compressibility were considered in the analysis. The authors reported that the magnitude of viscous dissipation is in the same order as the order of the wall heat flux and could not be neglected. Therefore, both viscous dissipation and rarefaction must be considered simultaneously to predict the heat transfer behavior. Dongari and Agrawal [24] reported the modeling of the Navier–Stokes equations with the conventional second order slip boundary condition at high Knudsen numbers by including the Knudsen diffusion phenomenon in rarefied gas flows. The authors consider the effect of thermal creep in rarefied gas flows through microdevices. In another study the authors [25] presented the solution of the gaseous slip flow in long microchannel with a second order slip boundary condition at the wall. It has been reported that thermal creep contribution mainly appears in the entrance region for the developing flow where higher tangential temperature gradients occur and vanish in the fully developed region. Cetin [26] reported the deviation in the Nusselt number by considering thermal creep is 1.63% and 3.71% compared to the Nusselt number without thermal creep for the case of $Kn = 0.04$ and 0.12, respectively. Studies have also been reported that consider the effect of thermal creep on heat transfer and fluid flow analysis in the developing region for an isoflux condition [27–29]. In addition, Demsis *et al* [30] evaluated the heat transfer coefficient of gaseous flows in the slip flow regime through an experimental investigation.

Efforts have been made to analyze the effect of viscous dissipation on the heat transfer characteristics of Newtonian fluid between two infinite parallel plates with asymmetric heat flux boundary conditions at the wall [31–36]. Zhu [32] reported the fluid flow and heat transfer characteristics of gaseous flows between parallel plates with unsymmetrical wall heat flux condition in the slip flow regime neglecting the effect of viscous dissipation. The heat transfer characteristics of plug flows through parallel plates and concentric annuli with asymmetric heat flux condition at the walls was reported by Shojaeian *et al* [33]. It was reported that the Nusselt number may increase or decrease depending on the parameters such as rarefaction, wall heat flux ratio and annulus aspect ratio. Kushwaha and Sahu [34] studied the sole effect of second order velocity slip on heat transfer characteristics of gaseous flows through parallel plates under different heat flux boundary conditions. Zhang *et al* [35] reported convective heat transfer characteristics of gaseous flow through a two dimensional microchannel in the slip region including the effects of velocity slip, temperature jump and viscous dissipation. The authors found that the Nusselt number decreases with the increase in the Brinkman number. Sadeghi and Saidi [36] presented forced convection heat transfer of gaseous flow through microannulus and parallel plate microchannel with asymmetric heat flux boundary conditions. The authors reported the effect of viscous dissipation on Nusselt number is insignificant at higher values of Knudsen number, while, in the absence of viscous dissipation Nusselt number decreases with the increase in Knudsen number.

It is evident from the literature that only a single investigation [36] has been reported that consider the effect of velocity slip, temperature jump, rarefaction and viscous dissipation by employing asymmetric heat flux boundary conditions at microscale. Therefore, further investigation is required to analyze the heat transfer and fluid flow in the slip flow region with asymmetric heat flux boundary condition. The objective of the present analytical investigation is to study the effect of asymmetric heat flux ratio, viscous dissipation and rarefaction on the fluid flow and heat transfer behavior of gaseous flow through parallel plates. In the previous study Kushwaha and Sahu [19, 20] considered the second order velocity slip and temperature jump to analyze the heat transfer behavior of gaseous flows through parallel plate microchannels with symmetric heating condition. The second order models are more accurate compared to first order models, while the models increase the mathematical complexity and do not yield the solution in the form of closed form expressions. Here, the first order velocity slip and temperature jump is used for the analysis. Closed form expressions are obtained for the temperature distribution and Nusselt number as a function of various modeling parameters. The effect of asymmetric heat flux ratio with and without viscous dissipation on Nusselt number for both macroscale and microscale is highlighted. The present prediction is validated for the case that neglects microscale effects ($Kn = 0$) and exhibits reasonably good agreement with other analytical results.

2. Theoretical analysis

The schematic of steady gaseous flow between infinite fixed parallel plates with different constant heat fluxes (q_1 and q_2) boundary conditions at the surface is shown in figure 1. Here, the plates are maintained at a distance of W apart in the transverse direction (figure 1). For the case of long channel and low speed flows (small pressure gradients), the flow is approximated as hydrodynamically and thermally fully developed; also, the flow is considered to be incompressible. It is argued that the fully developed Nusselt number is almost invariant for constant and variable properties cases because of reduced temperature gradients in this region [37]. In this study, the effect of property variation on the flow behavior is considered to be negligible. It is reported that thermal creep affects the slip velocity in the entrance region only and vanishes in the fully developed region, therefore, the effect of thermal creep is neglected here [26, 29]. It is argued that the effect of axial conduction is significant in the thermal entrance region and becomes small in the fully developed region [38]. Present study neglects the axial conduction in the analysis.

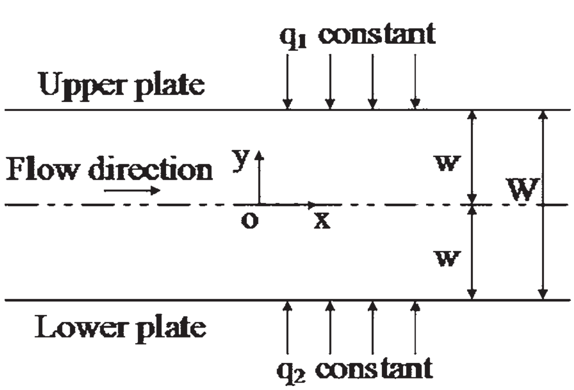

Figure 1. Schematic of parallel plates.

The heat transfer and fluid flow behavior through parallel plates is analyzed in the fully developed region and usual continuum approach is coupled with two main characteristics of the microscale phenomena i.e. velocity slip and temperature jump at the wall. Utilizing the above assumptions, the momentum equation can be written as

$$\frac{\mathrm{d}}{\mathrm{d}y}\left(\frac{\mathrm{d}u}{\mathrm{d}y}\right) = \frac{1}{\mu}\frac{\mathrm{d}p}{\mathrm{d}x} \tag{1}$$

Subjected to the following boundary conditions:

$$\left.\frac{\mathrm{d}u}{\mathrm{d}y}\right|_{y=0} = 0 \tag{2a}$$

$$u_s - u_w = -\frac{2-F}{F}\lambda\left.\frac{\mathrm{d}u}{\mathrm{d}y}\right|_{y=w} \tag{2b}$$

where u_s and u_w denote the velocity of fluid at the wall and the velocity of wall, respectively. Here, λ and F represent the mean free path and tangential momentum accommodation coefficient, respectively. The value of F can be taken as unity for air because its impact can be included in Kn [1–4]. The value of u_w is considered to be zero with respect to fixed reference frame.

The following dimensionless variables are defined:

$$X = \frac{x}{W}, \quad Y = \frac{y}{W}, \quad Kn = \frac{\lambda}{W} \tag{3}$$

The fully developed velocity profile for the slip flow can be derived from the momentum equation by using the first order velocity slip condition. Utilizing Eqs. (1)–(3) the velocity distribution as a function of transverse coordinate can be written as

$$\frac{u}{u_m} = \frac{3}{2}\left[\frac{1 + 4Kn - y^2/w^2}{1 + 6Kn}\right] \tag{4}$$

Utilizing the assumptions made in section 2, the energy equation can be written as

$$\rho u c_p \frac{\partial T}{\partial x} = k\frac{\partial^2 T}{\partial y^2} + \mu\left(\frac{\partial u}{\partial y}\right)^2 \tag{5}$$

Subject to the boundary conditions, given by

(i)

$$q_1 = k\left.\frac{\partial T}{\partial y}\right|_{y=w}, \quad T = T_1 \quad \text{at} \quad y = w \tag{6a}$$

(ii)

$$q_2 = -k\left.\frac{\partial T}{\partial y}\right|_{y=-w} \tag{6b}$$

Taking a cue from earlier analyses [9, 18, 26, 35, 36], the temperature jump at the wall can be written as

$$T_s - T_w = -\frac{2 - F_t}{F_t}\frac{2\gamma}{(\gamma + 1)}\frac{\lambda}{\Pr}\frac{\partial T}{\partial y}\bigg|_{y=w} \tag{7}$$

The value of thermal accommodation coefficient (F_t) is assumed to be unity in the present analysis. For the present configuration the flow is assumed to be fully developed and the axial temperature gradient is considered to be constant [1–4].

$$\frac{\partial T}{\partial x} = \frac{\mathrm{d}T_s}{\mathrm{d}x} = \frac{\mathrm{d}T_m}{\mathrm{d}x} \tag{8}$$

In order to solve the energy equation (Eq. 5), the axial temperature gradient can be obtained by applying the first law of thermodynamics to an elemental control volume as [1–4].

$$\frac{\mathrm{d}T_m}{\mathrm{d}x} = \frac{q''P + \int \mu\phi \mathrm{d}A}{mc_p} \tag{9}$$

The non-dimensionalized variables are defined as follows:

$$\alpha = \frac{k}{\rho c_p}, \quad Br_{q1} = \frac{\mu u_m^2}{q_1 W}, \quad \theta = \frac{T - T_1}{(q_1 W/k)}, \quad \theta_m = \frac{T_m - T_1}{(q_1 W/k)} \tag{10}$$

Utilizing Eqs. (4)–(6), the governing equation (Eq. 5) in dimensionless form can be written as

$$\frac{\mathrm{d}^2\theta}{\mathrm{d}Y^2} = \frac{3}{2}\frac{u_m}{\alpha}\frac{(1+4Kn-4Y^2)}{(1 + 6Kn)}\frac{kW}{q_1}\frac{\mathrm{d}T_1}{\mathrm{d}x} - \frac{144Br_{q1}Y^2}{(1 + 6Kn)^2} \tag{11}$$

Subject to the following boundary conditions:

$$\text{(i)} \quad \frac{\partial\theta}{\partial Y} = 1, \quad \theta = 0 \quad \text{at} \quad Y = \frac{1}{2} \tag{12a}$$

$$\text{(ii)} \quad \frac{\partial\theta}{\partial Y} = -\frac{q_2}{q_1} \quad \text{at} \quad Y = -\frac{1}{2} \tag{12b}$$

Utilizing Eqs. (11) and (12) one can obtain the temperature distribution as a function of transverse coordinate for the parallel plates and can be expressed as

$$\begin{aligned}\theta(Y) = &\frac{1}{2}\frac{1}{1 + 6Kn}\left(1 + \frac{q_2}{q_1}\right)\left(3 + \frac{18Br_{q1}}{(1 + 6Kn)^2}\right)\left(\frac{Y^2(1 + 4Kn)}{2} - \frac{Y^4}{3}\right)\\ &- \frac{12Br_{q1}Y^4}{(1 + 6Kn)^2} + Y\left(1 - \frac{1}{2}\left(1 + \frac{q_2}{q_1}\right)\left(1 + \frac{6Br_{q1}}{(1 + 6Kn)^2}\right) + \frac{6Br_{q1}}{(1 + 6Kn)^2}\right)\\ &- \frac{1}{32}\left(1 + \frac{q_2}{q_1}\right)\left(\frac{5 + 24Kn}{1 + 6Kn}\right)\left(1 + \frac{6Br_{q1}}{(1 + 6Kn)^2}\right)\\ &+ \frac{1}{4}\left(1 + \frac{q_2}{q_1}\right)\left(1 + \frac{6Br_{q1}}{(1 + 6Kn)^2}\right) - \frac{9Br_{q1}}{4(1 + 6Kn)^2} - \frac{1}{2}\end{aligned} \tag{13}$$

Utilizing Eq. (13), one can evaluate the temperature distribution of the fluid in transverse direction for the given value of Knudsen number (Kn), ratio of constant heat flux parameter (q_2/q_1) and modified Brinkman number (Br_{q1}).

In the case of an internal flow with heat transfer, the temperature of the fluid at any axial location of the duct varies in the transverse direction. In case of internal flow, the mean or bulk temperature (T_m) of the fluid is usually used to evaluate the heat transfer coefficient (Nusselt number). It may be noted that the mean or the bulk temperature T_m at a given cross section of the duct is defined on the basis of thermal energy transported by the fluid stream that passes through the given cross section and can be expressed as [3, 4]:

$$T_m = \frac{\int \rho uT\mathrm{d}A}{\int \rho u\mathrm{d}A} \tag{14}$$

It may be noted that for the case of $Kn = 0$, and $Br_{q1} = 0$, present prediction (Eq. 13) reduces to Eq. (15) and it is identical to that obtained by the researchers [9, 18, 31, 32, 35, 36].

$$\theta(Y) = -\frac{Y^4}{3}\left(\frac{3}{2} + \frac{3q_2}{2q_1}\right) + \frac{Y^2}{2}\left(\frac{3}{2} + \frac{3q_2}{2q_1}\right) + Y\left(\frac{1}{2} - \frac{1}{2}\frac{q_2}{q_1}\right) + \frac{3}{32}\frac{q_2}{q_1} - \frac{13}{32} \tag{15}$$

Using Eqs. (4), (13) and (14), the bulk mean temperature (θ_m) is obtained as

$$\begin{aligned}\theta_m = &-\frac{3}{1120}\left(1 + \frac{q_2}{q_1}\right)\frac{1 + 14Kn}{(1 + 6Kn)^2}\left(1 + \frac{6Br_{q1}}{(1 + 6Kn)^2}\right)\\ &+ \frac{3}{80}\left(1 + \frac{q_2}{q_1}\right)\frac{(1 + 14Kn)(1 + 10Kn)}{(1 + 6Kn)^2}\left(1 + \frac{6Br_{q1}}{(1 + 6Kn)^2}\right)\\ &- \frac{9Br_{q1}(1 + 14Kn)}{140(1 + 6Kn)^3} + \frac{1}{4}\left(1 + \frac{q_2}{q_1}\right)\left(1 + \frac{6Br_{q1}}{(1 + 6Kn)^2}\right)\\ &- \frac{9Br_{q1}}{4(1 + 6Kn)^2} - \frac{1}{32}\left(1 + \frac{q_2}{q_1}\right)\left(1 + \frac{6Br_{q1}}{(1 + 6Kn)^2}\right)\left(\frac{5 + 24Kn}{1 + 6Kn}\right) - \frac{1}{2}\end{aligned} \tag{16}$$

Utilizing Eq. (7) and Eq. (16) the temperature in dimensionless form can be expressed as

$$\begin{aligned}\theta_m^* = &-\frac{3}{1120}\left(1 + \frac{q_2}{q_1}\right)\frac{1 + 14Kn}{(1 + 6Kn)^2}\left(1 + \frac{6Br_{q1}}{(1 + 6Kn)^2}\right)\\ &+ \frac{3}{80}\left(1 + \frac{q_2}{q_1}\right)\frac{(1 + 14Kn)(1 + 10Kn)}{(1 + 6Kn)^2}\left(1 + \frac{6Br_{q1}}{(1 + 6Kn)^2}\right)\\ &- \frac{9Br_{q1}(1 + 14Kn)}{140(1 + 6Kn)^3} + \frac{1}{4}\left(1 + \frac{q_2}{q_1}\right)\left(1 + \frac{6Br_{q1}}{(1 + 6Kn)^2}\right) - \frac{9Br_{q1}}{4(1 + 6Kn)^2}\\ &- \frac{1}{32}\left(1 + \frac{q_2}{q_1}\right)\left(1 + \frac{6Br_{q1}}{(1 + 6Kn)^2}\right)\left(\frac{5 + 24Kn}{1 + 6Kn}\right) - \frac{2Kn\gamma}{\Pr(1 + \gamma)}\frac{q_2}{q_1} - \frac{1}{2}\end{aligned} \tag{17}$$

For the case of $Kn = 0$, the bulk mean temperature obtained by present analysis (Eq. 16) is identical to that derived by the researchers [9, 18, 31, 32, 35, 36].

$$\theta_m = \left[\frac{9}{70}\frac{q_2}{q_1} - \frac{13}{35} - \frac{27}{35}Br_{q1}\right] \tag{18}$$

The Nusselt number is defined as [9, 18, 31, 32, 35, 36]:

$$Nu = \frac{hW}{k} \quad or \quad \frac{q_1}{T_1 - T_m}\frac{W}{k} \Rightarrow -\frac{1}{\theta_m^*}\frac{d\theta}{dY}\bigg|_{wall} \tag{19}$$

Utilizing Eq. (17) and Eq. (19), the Nusselt can be written as

$$Nu = -\begin{bmatrix} -\frac{3}{1120}\left(1+\frac{q_2}{q_1}\right)\frac{1+14Kn}{(1+6Kn)^2}\left(1+\frac{6Br_{q1}}{(1+6Kn)^2}\right) \\ +\frac{3}{80}\left(1+\frac{q_2}{q_1}\right)\frac{(1+14Kn)(1+10Kn)}{(1+6Kn)^2}\left(1+\frac{6Br_{q1}}{(1+6Kn)^2}\right) \\ -\frac{9Br_{q1}(1+14Kn)}{140(1+6Kn)^3}+\frac{1}{4}\left(1+\frac{q_2}{q_1}\right)\left(1+\frac{6Br_{q1}}{(1+6Kn)^2}\right) \\ -\frac{9Br_{q1}}{4(1+6Kn)^2}-\frac{1}{32}\left(1+\frac{q_2}{q_1}\right)\left(1+\frac{6Br_{q1}}{(1+6Kn)^2}\right)\left(\frac{5+24Kn}{1+6Kn}\right) \\ -\frac{2Kn\gamma}{\Pr(1+\gamma)}\frac{q_2}{q_1}-\frac{1}{2} \end{bmatrix}^{-1} \tag{20}$$

From the analysis, a closed form expression is obtained for the Nusselt number as a function of various parameters such as: modified Brinkman number, Knudsen number, the ratio of different heat fluxes and ratio of specific heats (Eq. 20). It may be noted that Eq. (20) reduces to Eq. (21) for the case of $Kn = 0$ and is identical to that derived by the researchers [9, 18, 31, 32, 35, 36].

$$Nu = \left[\frac{70}{26 - 9\frac{q_2}{q_1} + 54Br_{q1}}\right] \tag{21}$$

For the case that considers equal heat fluxes for both the upper and lower plates, Eq. (21) reduces to Eq. (22).

$$Nu = \left[\frac{70}{17 + 54Br_{q1}}\right] \tag{22}$$

For the case of $q_1 = q_2$ and $Br_{q1} = 0$, present prediction ($Nu = 70/17$) is exactly same as obtained by the researchers [9, 18, 31, 32, 35, 36].

3. Results and discussion

3.1 *Comparison and validation*

In this study attempts have been made to compare present predictions with other models [9, 18, 28, 35] for symmetric heat flux ratio ($q_2/q_1 = 1$) and various modified Brinkman number (0, 0.01, −0.01) and is shown in tables 1–3. The results obtained by Aydin and Avci [9], Tunc and Bayazitoglu [18], Sun *et al* [28], Zhang *et al* [35] and present prediction are shown in tables 1–3. For $Kn = 0$, all previous analytical results agree closely with the present solution. The agreement becomes poor with the increase in Knudsen number. It is interesting to note that the agreement between various reported models weakens with the increase in the Knudsen number. A comparison among various studies such as Aydin and Avci [9], analytical model of Inman [15], Hooman [16], Miyamoto *et al* [21], DSMC solution of Balaj *et al* [22], and the present prediction for the case of positive

Table 1. Comparison of the Nusselt number at $Pr = 0.7$, $Br_{q1} = 0$, $q_2/q_1 = 1$.

Kn	Present	Aydin and Avci [9]	Tunc and Bayazitoglu [18]	Sun *et al* [28]	Zhang *et al* [35]
0.00	4.118	4.118	4.118	4.365	4.118
0.02	3.735	3.750	3.750	4.109	3.979
0.04	3.395	3.421	3.421	3.804	3.739
0.06	3.098	3.131	3.131	3.499	3.582
0.08	2.842	2.878	2.878	3.216	3.374
0.10	2.619	2.657	2.657	2.962	3.226

Table 2. Comparison of the Nusselt number at $Pr = 0.7$, $Br_{q1} = 0.01$, $q_2/q_1 = 1$.

Kn	Present	Aydin and Avci [9]	Tunc and Bayazitoglu [18]	Sun *et al* [28]	Zhang *et al* [35]
0.00	4.011	4.078	4.086	4.183	4.051
0.02	3.642	3.725	3.729	4.002	3.914
0.04	3.314	3.405	3.405	3.740	3.724
0.06	3.027	3.120	3.119	3.459	3.566
0.08	2.779	2.869	2.869	3.191	3.344
0.10	2.564	2.652	2.651	2.945	3.196

Table 3. Comparison of the Nusselt number at $Pr = 0.7$, $Br_{q1} = -0.01$, $q_2/q_1 = 1$.

Kn	Present	Aydin and Avci [9]	Tunc and Bayazitoglu [18]	Sun *et al* [28]	Zhang *et al* [35]
0.00	4.281	4.442	4.748	4.564	4.188
0.02	3.876	4.146	4.289	4.221	3.973
0.04	3.517	3.784	3.879	3.869	3.804
0.06	3.206	3.454	3.934	3.539	3.635
0.08	2.937	3.149	3.207	3.242	3.402
0.10	2.704	2.952	2.938	2.978	3.233

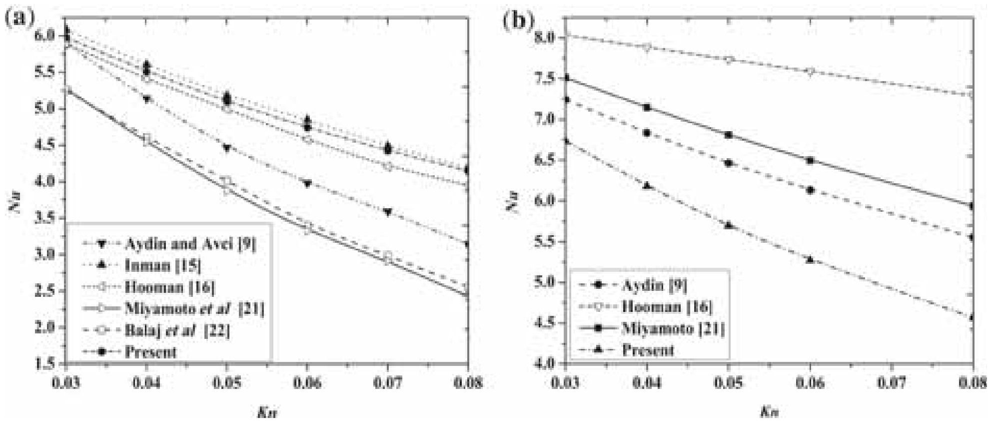

Figure 2. Comparison of Nusselt number for positive and negative values of Brinkman number.

value of Brinkman number shown in figure 2a. Figure 2b depicts the comparison of present prediction for the case of negative value of Brinkman number with the results obtained by various models namely, Aydin and Avci [9], Hooman [16] and Miyamoto *et al* [21]. It may be noted that the Nusselt number is found to decrease with the Knudsen number in the case of positive and negative values of Brinkman number. The results are presented for argon gas ($Pr = 2/3$, $\gamma = 5/3$). For the case of positive Brinkman number, present prediction exhibits reasonably good agreement with the model of Inman [15] and Hooman [16] as shown in figure 2a. While the results by Miyamoto *et al* [21] and the DSMC simulation [22] predict lower value of Nusselt number compared to present prediction, the model of Aydin and Avci [9], Inman [15] and Hooman [16]. It is observed that analytical solutions and the DSMC solution reported by various researchers do not match with each other. This may be due to the different solution methodology and assumptions adopted in their study. While, in the case of negative Brinkman number, present model exhibits lower value of Nusselt number compared to results obtained by Miyamoto *et al* [21], Aydin and Avci [9] and Hooman [16] as shown in figure 2b.

3.2 *Parametric variation*

In this study an attempt has been made to investigate the effect of viscous dissipation, heat flux ratio and rarefaction on fluid flow and heat transfer characteristics of hydrodynamically and thermally fully developed flow between parallel plates. Here, the upper and lower plates are subjected to different constant heat fluxes q_1 and q_2, respectively. In this study, air is considered as working fluid and results are obtained by using constant values of $Pr = 0.7$ and $\gamma = 1.4$. The results are presented for Knudsen number within the range of 10^{-3} to 10^{-1}, heat flux ratio within the range of 1–5 and for a wide range of modified Brinkman number. It may be noted that for the given range of Knudsen number ($0.001 < Kn < 0.10$), the hydraulic diameter of a microchannel can be obtained in the slip flow range. From the analysis, closed form expressions are obtained for the temperature distribution and Nusselt number. The present prediction is validated for the case that neglects viscous heating ($Br_{q1} = 0$) and microscale effects ($Kn = 0$). The Nusselt number for $Kn = 0$ is found to be exactly same as reported by earlier researchers [9, 18, 31, 32, 35, 36].

The effect of asymmetric heat flux ratio on temperature profile that consider no viscous heating and no rarefaction effect ($Br_{q1} = 0$, $Kn = 0$) is depicted in figure 3a. It is observed that asymmetric heat flux ratio alters the variation in temperature profile and the difference in temperature between upper and lower plate increases with the increase in asymmetric heat flux ratio. Figure 3b depicts the variation in temperature distribution that considers viscous dissipation and no rarefaction effect ($Br_{q1} = 0.1$, $Kn = 0$). By

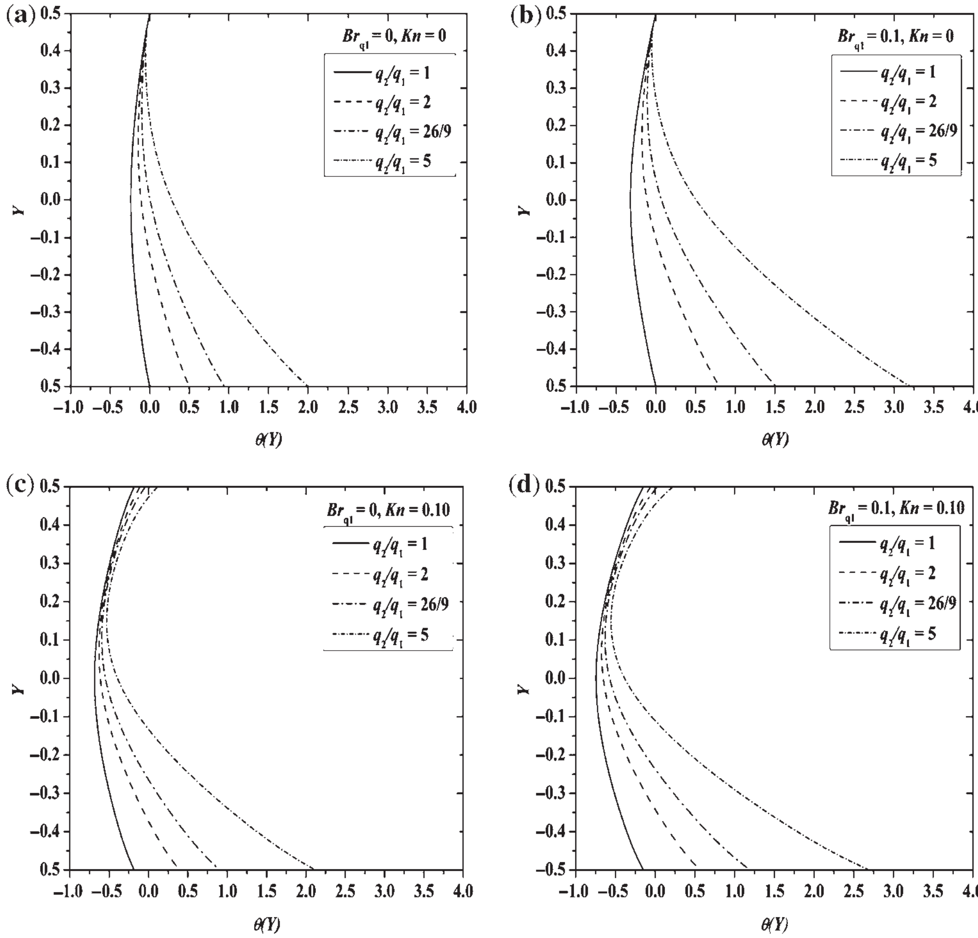

Figure 3. (**a**)–(**d**) Effect of Kn and Br_{q1} on temperature distribution for different heat flux ratios.

considering viscous dissipation, it is observed that the difference in temperature between upper and lower plate increases significantly with the increase in asymmetric heat flux ratio. For the case that considers viscous dissipation, the difference in temperature between upper and lower plate is found to be 1.6 times higher compared to the case that neglects viscous dissipation in the model (figure 3a–b). This indicates that in the presence of viscous dissipation, the asymmetric heat flux ratio severely affects the temperature profile in case of parallel plates. The effect of asymmetric heat flux ratio on the temperature profile for the case that neglects viscous dissipation and considers rarefaction ($Br_{q1} = 0$, $Kn = 0.10$) and the one considers both rarefaction and viscous dissipation ($Br_{q1} = 0.1$, $Kn = 0.10$) is depicted in figure 3c and figure 3d, respectively. It is noticed that asymmetric heat flux ratio alters the variation in temperature profile. The case that neglects viscous dissipation and considers rarefaction ($Br_{q1} = 0$, $Kn = 0.10$) exhibits significant temperature difference compared to the case that considers both rarefaction and viscous dissipation ($Br_{q1} = 0.1$, $Kn = 0.10$).

The ratio of heat generation because of viscous dissipation and the heat exchange between the fluid and the wall is characterized by the modified Brinkman number. Positive values of the modified Brinkman number correspond to the wall heating case that indicates the heat transfer from wall to the fluid, while the opposite is true for the negative modified Brinkman number [9, 32, 35]. The effect of the Knudsen number on the temperature distribution for different values of the modified Brinkman number and heat flux ratio is shown in figure 4a–c. Figure 4a shows the variation in temperature with Knudsen number for the case of no viscous dissipation. It is observed that with the increase in Knudsen number, the temperature jump at the heated wall increases leading to a decrease in the temperature. Further, the variation in temperature with Knudsen number in the presence of both positive and negative values of Brinkman number is shown in figure 4b–c. It is observed that the slope of the temperature is highest for the case of negative value of modified Brinkman number ($Br_{q1} = -0.1$), while the slope decreases gradually for the case of $Br_{q1} = 0$ and $Br_{q1} = 0.1$. This indicates that for a given Knudsen number, the heat transfer is highest in the case of negative Brinkman number and gradually decreases as the modified Brinkman number is increased from 0 to 0.1. The viscous dissipation is found to increase the bulk

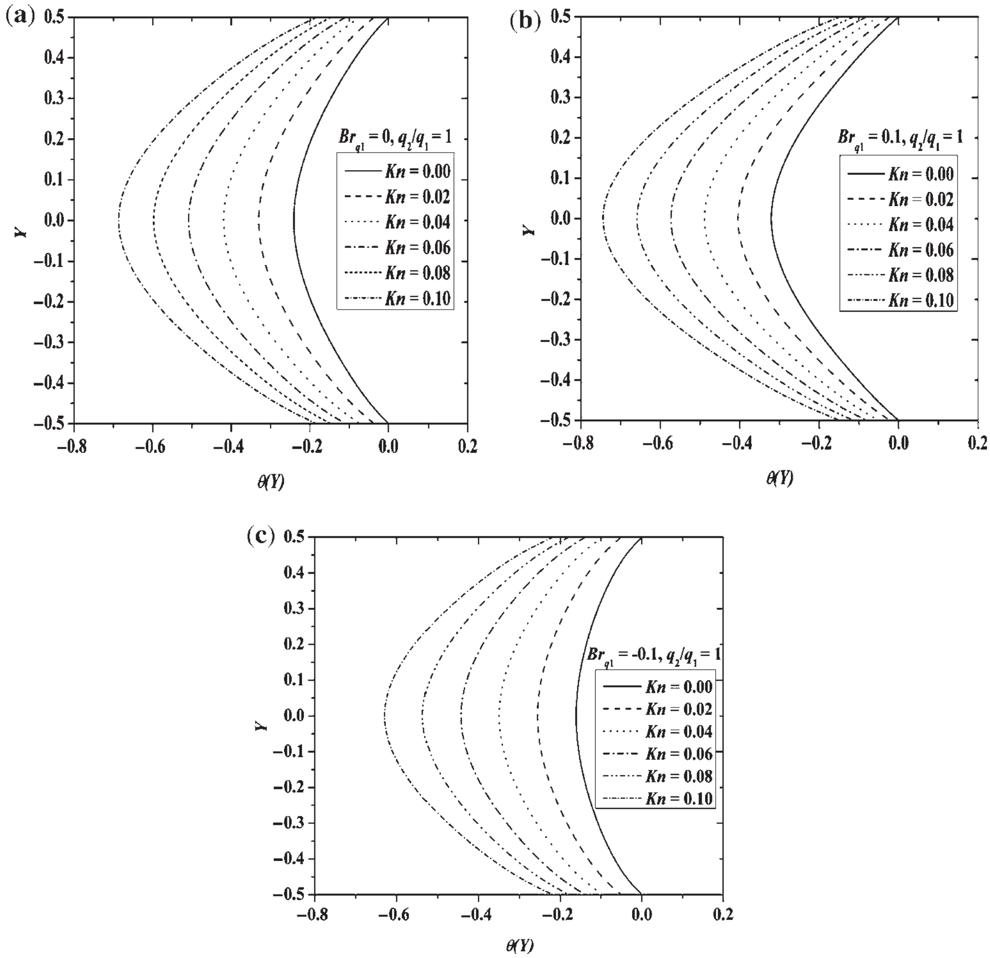

Figure 4. (**a**)–(**c**) Effect of Kn on temperature distribution at different modified Brinkman number for the case of $q_2/q_1 = 1$.

temperature because of internal heating of the fluid. Consequently, it reduces the temperature difference between the fluid and wall for positive value of the modified Brinkman number (figure 4b). In the case of negative value of the modified Brinkman number, heat transfer occurs from fluid to wall leading to a decrease in bulk temperature of the fluid, while viscous dissipation increases the temperature of the fluid (figure 4c).

Figure 5a–c demonstrates the effect of higher heat flux ratio in the presence of rarefaction (Kn) and viscous dissipation on temperature distribution. The results are presented for various modified Brinkman numbers ($Br_{q1} = 0$, 0.1, -0.1), Knudsen number (0–0.10) and $q_2/q_1 = 5$. Here, the extreme points of the temperature distribution at the lower wall are found to move towards the positive or negative direction with the increase in Knudsen number. In all the cases the temperature profile is severely distorted for the given modified Brinkman number and heat flux ratio with the varying Knudsen number range. Similar results have been reported by earlier researchers [9, 18, 31, 32, 35, 36]. The variation of temperature for various modified Brinkman number ($Br_{q1} = -0.1$, -0.01, 0, 0.01, 0.1) and Knudsen number ($Kn = 0$, 0.06, 0.1) is shown in figure 6a–c. It is observed that for positive values of the modified Brinkman number the wall temperatures are greater than the bulk temperature. The difference between the wall and the bulk temperature increases with increase in the modified Brinkman number. It is observed that, for a given value of the Knudsen number, the fluid temperature attains same value at a fixed transverse location irrespective of the modified Brinkman number for various Knudsen number. For a given value of heat flux ratio ($q_2/q_1 = 1$), the transverse locations are found to be at $Y = \pm 0.3964$ and $Y = \pm 0.3974$ for $Kn = 0.06$ and 0.10, respectively.

Figure 7a–c demonstrates the variation of Nusselt number with the modified Brinkman number for various heat flux ratios ($q_2/q_1 = 0$, 1, 26/9, 5) and Knudsen number ($Kn = 0$, 0.06, 0.10). For the case of no rarefaction effect ($Kn = 0$), the Nusselt number decreases with the increase in modified Brinkman number (figure 7a). It is observed that the variation of Nusselt number with modified Brinkman number is not continuous and singular points are observed at different Br_{q1} for each Knudsen number. From

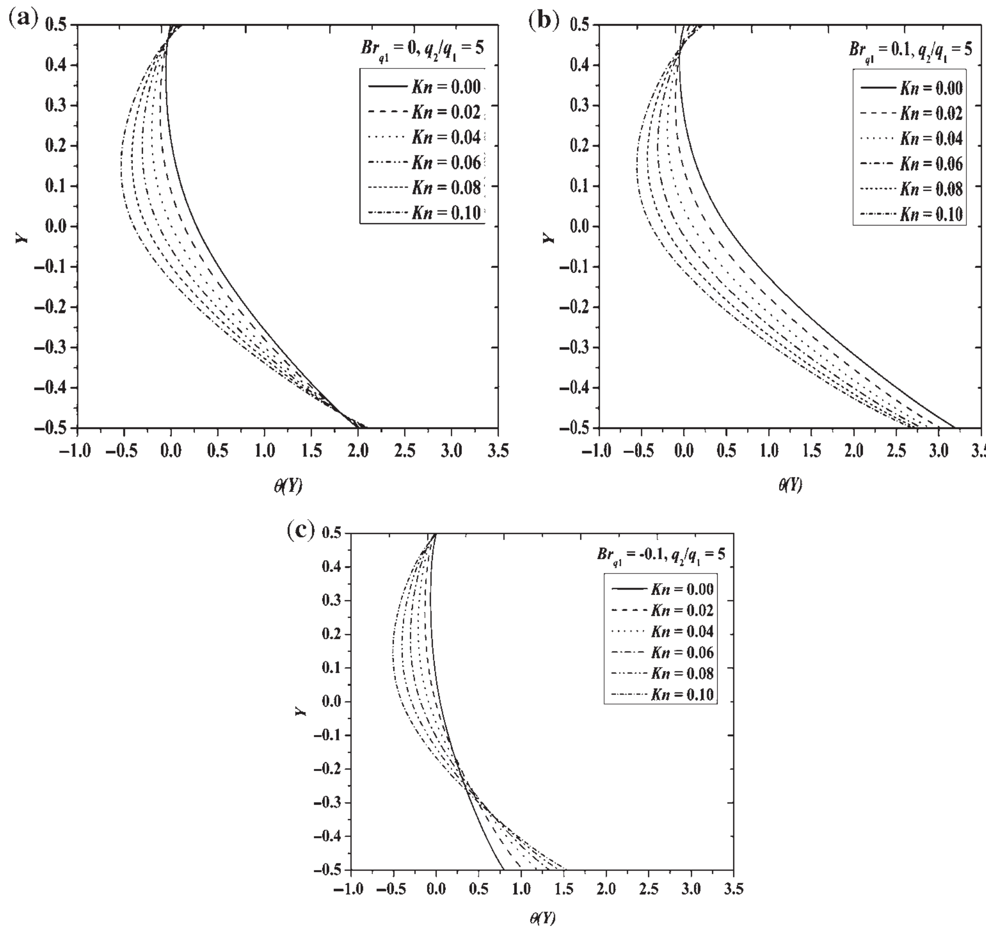

Figure 5. (**a**)–(**c**) Effect of Kn on temperature distribution at different modified Brinkman number for the case of $q_2/q_1 = 5$.

the analysis, we have presented the mathematical expression among various modeling parameters and expressed in Eq. (18). Using Eq. (18), one can evaluate the point of singularity at different modified Brinkman number, Knudsen number and heat flux ratio. For $Kn = 0$, the singular points for $q_2/q_1 = 1$ and 26/9 are obtained at $Br_{q1} = 0.286$ and 0.0001, respectively. The variation in Nusselt number variation for $Kn = 0.06$ and 0.10 is shown in figure 7b–c. For $Kn = 0.06$, the onset of singularity for various heat flux ratios $q_2/q_1 = 1$, 26/9, 5 is observed at $Br_{q1} = 1.891$, 1.263, 1.155, respectively (figure 7b). While, for $Kn = 0.10$, the onset of singularity for various heat flux ratios $q_2/q_1 = 1$, 26/9, 5 can be obtained at $Br_{q1} = 3.724$, 2.764, 2.593 (figure 7c). It may be observed from the figures that the onset of the point of singularity is altered with the inclusion of rarefaction effect and viscous dissipation. The point of singularity essentially signifies the balance between the heat generated due to viscous dissipation and the heat supplied by wall to the fluid. Therefore, for a given heat flux ratio (q_2/q_1), there could be a particular value of modified Brinkman number for which the fluid temperature (due to viscous heating) may become equal to the wall temperature. In such a case, no heat transfer takes place in either direction and results in an unbounded swing in the Nusselt number as seen in figure 7a–c.

The effect of various parameters such as Knudsen number, heat flux ratio and modified Brinkman number on Nusselt number is presented in tables 4–7. Table 4 presents a comparison of present results for the case of $q_2/q_1 = 0$, $Br_{q1} = 0$ and $0.001 < Kn < 0.1$. For the case of no viscous dissipation ($Br_{q1} = 0$, $Kn = 0$), the difference in Nusselt number between the cases such as $q_2/q_1 = 2$ and $q_2/q_1 = 1$ is found to be 52.94%. While for the case of ($Br_{q1} = 0$, $Kn = 0.1$), the difference in Nusselt number between these two cases reduced to 37.50%. This indicates that the change in Nusselt number because of change in heat flux ratio is significant in macroscale ($Kn = 0$) compared to the microscale ($Kn = 0.10$) in the absence of viscous dissipation. Similar observations have been made for $q_2/q_1 = 0$ and $q_2/q_1 = 1$ as shown in table 4. Also, an attempt has been made to evaluate the effect of heat flux ratio considering both viscous dissipation and rarefaction effect and is shown in tables 5 and 6. For $Br_{q1} = 0.01$ and $Kn = 0$, the difference in Nusselt number between two cases such as $q_2/$

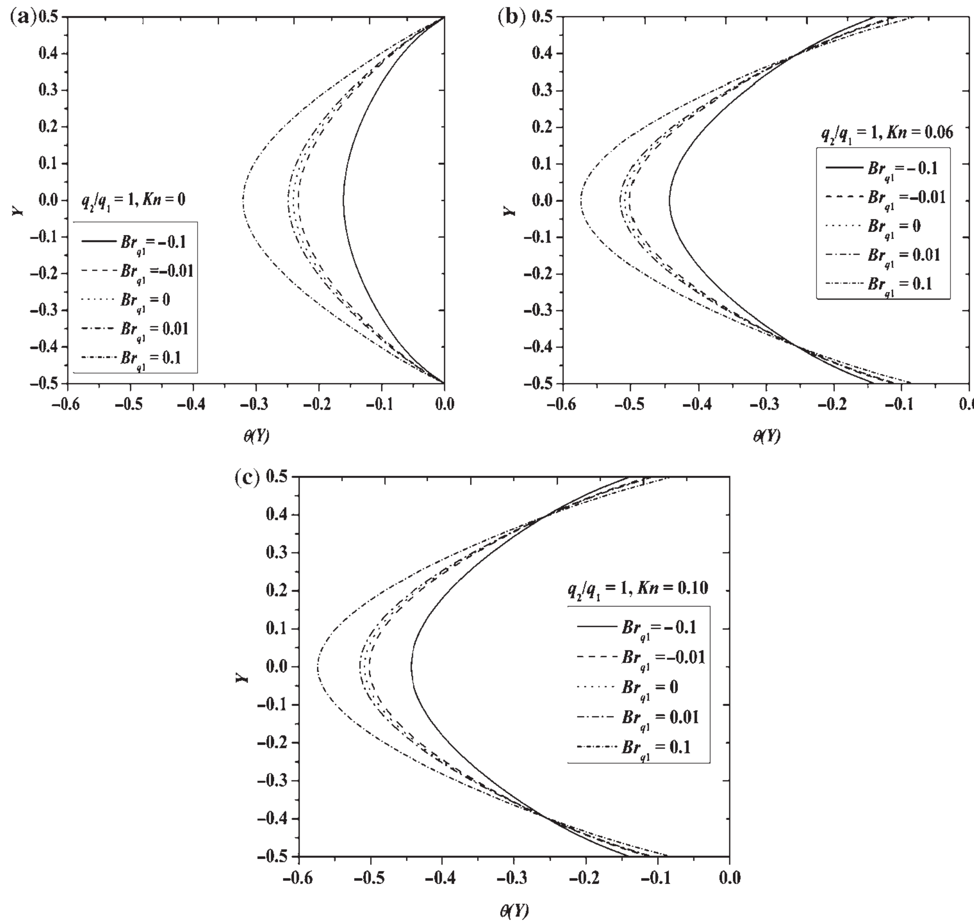

Figure 6. (**a**)–(**c**) Effect of Br_{q1} on temperature distribution at different Knudsen number for the case of $q_2/q_1 = 1$.

$q_1 = 2$ and $q_2/q_1 = 1$ is found to be 51.56%. While for the case of $Br_{q1} = 0.01$ and $Kn = 0.10$, the difference in Nusselt number between these two cases reduced to 36.52%. This indicates that the change in Nusselt number because of the change in heat flux ratio is significant in macroscale ($Kn = 0$) compared to the microscale ($Kn = 0.10$) with viscous dissipation as well. Similar observations have been made for various heat flux ratios such as $q_2/q_1 = 0$ and $q_2/q_1 = 1$ as shown in table 4. Also, for the case of negative value of modified Brinkman number ($Br_{q1} = -0.01$), the change in Nusselt number because of the change in heat flux ratio is significant in macroscale ($Kn = 0$) compared to the microscale ($Kn = 0.10$). Similar results have been reported by Zhang *et al* [35]. For the case of symmetric heat flux ratio ($q_2/q_1 = 1$, $Kn = 0$), the difference in Nusselt number between the cases such as $Br_{q1} = 0$ and $Br_{q1} = 0.01$ is found to be 2.59%. While for the case of $q_2/q_1 = 1$, $Kn = 0$, the difference in Nusselt number between these two cases reduces to 2.13%. The influence of viscous dissipation on Nusselt number for various values of Knudsen number is found to be insignificant.

4. Conclusions

In this study an analytical investigation has been carried out to evaluate the heat transfer and fluid flow characteristics in slip flow region for hydrodynamically and thermally fully developed flow between parallel plates. Here, the effect of first order velocity slip, temperature jump, viscous dissipation and asymmetric heat flux ratio are considered in the analysis. Closed form expressions are obtained for the temperature distribution and Nusselt number. Present predictions are verified for the cases that neglect the viscous heating and microscale effects. Based on the analysis following conclusions have been made and elaborated below.

- The viscous dissipation is found to distort the temperature distribution, significantly.
- The heat transfer characteristics are found to depend on various modeling parameters, namely, modified Brinkman number, Knudsen number and heat flux ratio.
- The variation in Nusselt number with the modified Brinkman number is not continuous and singularities are observed at different modified Brinkman number for each Knudsen number.

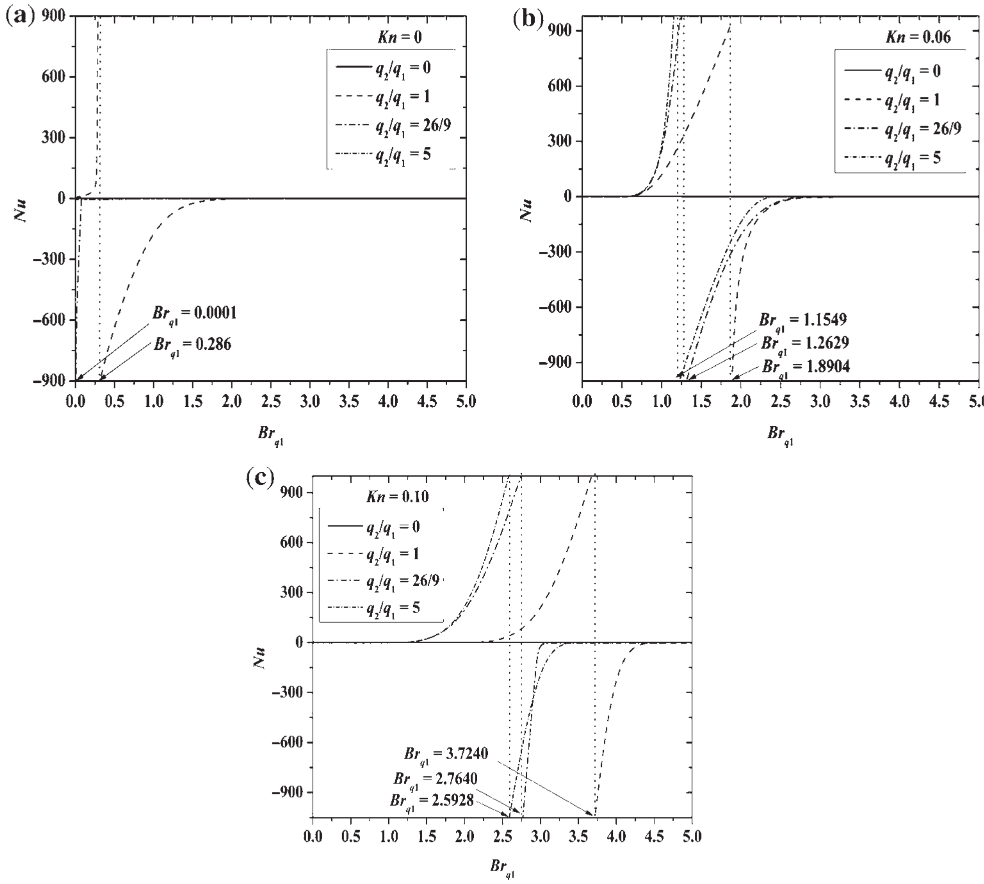

Figure 7. (**a**)–(**c**) Variation of the Nusselt number with modified Brinkman number.

Table 4. Percentage variation of the Nusselt number at $Br_{q1} = 0$.

	Present				
Kn	(a) $q_2/q_1 = 1$	(b) $q_2/q_1 = 2$	(c) $q_2/q_1 = 0$	(b − a/b) × 100	(a − c/a) × 100
0.00	4.118	8.750	2.692	52.94	34.63
0.02	3.735	7.408	2.496	49.58	33.17
0.04	3.395	6.307	2.322	46.17	31.61
0.06	3.098	5.431	2.167	42.96	30.05
0.08	2.842	4.736	2.030	39.99	28.57
0.10	2.612	4.179	1.908	37.50	26.95

- For a given asymmetric heat flux ratio, onset of singularity point shifts towards the higher value of modified Brinkman number with the increase in Knudsen number and heat flux ratio.
- The variation in Nusselt number because of the change in heat flux ratio is significant at macroscale ($Kn = 0$) compared to the case of microscale ($Kn = 0.10$) for both the cases i.e. with or without viscous dissipation.
- For a given heat flux ratio, the influence of viscous dissipation on Nusselt number is found to be insignificant at higher values of Knudsen number.

Nomenclature

Br_{q1}	modified Brinkman number, defined in Eq. (10)
c_p	specific heat at constant pressure, J/kg-K
h	convective heat transfer coefficient, W/m^2-K
k	thermal conductivity, W/m-K
Kn	Knudsen number, λ/W
L	width of the plate, m
Nu	Nusselt number
q_1	upper wall heat flux, W/m^2
q_2	lower wall heat flux, W/m^2

Table 5. Percentage variation of the Nusselt number at $Br_{q1} = 0.01$.

Kn	Present				
	(a) $q_2/q_1 = 1$	(b) $q_2/q_1 = 2$	(c) $q_2/q_1 = 0$	(b − a/b) × 100	(a − c/a) × 100
0.00	4.011	8.281	2.646	51.56	34.03
0.02	3.642	7.051	2.455	48.35	32.59
0.04	3.314	6.033	2.284	45.07	31.08
0.06	3.027	5.217	2.132	41.98	29.56
0.08	2.779	4.564	1.998	39.11	28.10
0.10	2.564	4.039	1.878	36.52	26.76

Table 6. Percentage variation of the Nusselt number at $Br_{q1} = -0.01$.

Kn	Present				
	(a) $q_2/q_1 = 1$	(b) $q_2/q_1 = 2$	(c) $q_2/q_1 = 0$	(b − a/b) × 100	(a − c/a) × 100
0.00	4.281	9.524	2.762	55.05	35.48
0.02	3.876	7.987	2.559	51.47	33.98
0.04	3.517	6.745	2.379	47.86	32.36
0.06	3.206	5.771	2.219	44.45	30.79
0.08	2.937	5.006	2.078	41.33	29.25
0.10	2.704	4.399	1.952	38.53	27.81

Table 7. Percentage variation of viscous dissipation effect on Nu for the case of $q_2/q_1 = 1$.

Kn	(a) $Br_{q1} = 0$	(b) $Br_{q1} = 0.01$	(c) $Br_{q1} = 0.1$	((b − a)/a) × 100	((a − c)/a) × 100	((b − c)/b) × 100
0.00	4.118	4.011	3.821	2.597	7.197	4.722
0.02	3.735	3.642	3.476	2.487	6.903	4.529
0.04	3.395	3.314	3.170	2.383	6.627	4.348
0.06	3.098	3.027	2.901	2.289	6.376	4.183
0.08	2.842	2.779	2.667	2.205	6.152	4.037
0.10	2.619	2.564	2.464	2.131	5.955	3.907

T temperature, K
T_1 upper wall temperature, K
T_2 lower wall temperature, K
T_s surface temperature, K
T_w fluid temperature at the wall, K
u velocity, m/s
u_m mean velocity, m/s
u_w wall velocity, m/s
u_s slip velocity $\left(= -\frac{2-F}{F}\lambda\frac{\partial u}{\partial y}\Big|_{y=w}\right)$, m/s
U dimensionless velocity
w half channel height, m
W channel height (=2w), m
x co-ordinate in the axial direction, m
y co-ordinate in the vertical direction, m
Y dimensionless vertical co-ordinate

Greek symbols

α thermal diffusivity, m^2/s
θ dimensionless temperature
θ_m mean dimensionless temperature
λ molecular mean free path, m
μ dynamic viscosity, kg/m-s
ρ density, kg/m^3

Subscripts

s properties at the surface
m mean

References

[1] Gad-el-Hak M Eds. *The MEMS handbook.* CRC Press, New York 2001

[2] Karniadakis G E and Beskok A 2002 *Micro flows: Fundamentals and simulation.* Springer-Verlag, New York

[3] Shah R K and London A L 1978 *Laminar flow forced convection in ducts: A source book for compact heat exchanger analytical data.* Academic Press, New York

[4] Kays W M, Crawford M E and Weigand B 2012 *Convective heat and mass transfer*. Tata McGraw-Hill

[5] Tso C P and Mahulikar S P 2000 Experimental verification of the role of Brinkman number in microchannels using local parameters. *Int. J. Heat Mass Transf.* 43: 1837–1849. doi:10.1016/S0017-9310(99)00241-0

[6] Aydin O 2005 Effects of viscous dissipation on the heat transfer in forced pipe flow. Part 1: Both hydrodynamically and thermally fully developed flow. *Energy Convers. Manag*. 46: 757–769. doi:10.1016/j.enconman.2004.05.004

[7] Aydin O 2005 Effects of viscous dissipation on the heat transfer in a forced pipe flow. Part 2: Thermally developing flow. *Energy Convers. Manag*. 46: 3091–3102. doi:10.1016/j.enconman.2005.03.011

[8] Aydın O and Avcı M 2006 Laminar forced convection with viscous dissipation in a Couette–Poiseuille flow between parallel plates. *Appl. Energy* 83: 856–867. doi:10.1016/j.apenergy.2005.08.005

[9] Aydın O and Avcı M 2007 Analysis of laminar heat transfer in micro-Poiseuille flow, *Int. J. Therm. Sci.* 46: 30–37. doi:10.1016/j.ijthermalsci.2006.04.003

[10] Morini G L and Spiga M 2007 The role of viscous dissipation in heated microchannels, *J. Heat Transf.* 120: 308–318. doi:10.1115/1.2430725

[11] Morini G L 2005 Viscous heating in liquid flows in microchannels. *Int. J. Heat Mass Transf.* 48: 3637–3647. doi:10.1016/j.ijheatmasstransfer.2005.01.011

[12] Giudice S D, Nonino C and Savino S 2007 Effects of viscous dissipation and temperature dependent viscosity in thermally and simultaneously developing laminar flows in microchannels, *Int. J. Heat Fluid Flow* 28: 15–27. doi:10.1016/j.ijheatfluidflow.2006.05.007

[13] Koo J and Kleinstreuer C. 2004 Viscous dissipation effects in microtubes and microchannels, *Int. J. Heat Mass Transf*. 47: 3159–3169. doi:10.1016/j.ijheatmasstransfer.2004.02.017

[14] Hossainpour S and Khadem M H 2010 Investigation of fluid flow and heat transfer characteristics of gases in microchannels with consideration of different roughness shapes at slip flow regime. *Nanoscale Microscale Thermophys. Eng*. 14(3): 137–151. doi:10.1080/15567265.2010.500317

[15] Inman R 1964 Laminar slip flow heat transfer in a parallel plate channel or a round tube with uniform wall heating. *NASA Technical Note D*-2393

[16] Hooman K 2007 Entropy generation for microscale forced convection: Effects of different thermal boundary conditions, velocity slip, temperature jump, viscous dissipation, and duct geometry. *Int. J. Heat Mass Transf.* 34: 945–957. doi:10.1016/j.icheatmasstransfer.2007.05.019

[17] Rij J V, Ameel T A and Harman T 2009 The effect of viscous dissipation and rarefaction on rectangular microchannel convective heat transfer. *Int. J. Therm. Sci*. 48: 271–281. doi:10.1016/j.ijthermalsci.2008.07.010

[18] Tunc G and Bayazitoglu Y 2001 Heat transfer in microtubes with viscous dissipation. *Int. J. Heat Mass Transf.* 44: 2395–2403. doi:10.1016/S0017-9310(00)00298-2

[19] Kushwaha H M and Sahu S K 2014 Analysis of gaseous flow in a micropipe with second order velocity slip and temperature jump boundary conditions. *Heat Mass Transf.* 50(12): 1649–1659. doi:10.1007/s00231-014-1368-3

[20] Kushwaha H M and Sahu S K 2013 Analysis of gaseous flow between parallel plates by second order velocity slip and temperature jump boundary conditions. *Heat Transf. Asian Res*. doi:10.1002/htj.21116

[21] Miyamoto M, Shi W, Katoh Y and Kurima J 2003 Choked flow and heat transfer of low density gas in a narrow parallel plate channel with uniformly heating walls. *Int. J. Heat Mass Transf.* 46: 2685–2693. doi:10.1016/S0017-9310(03)00030-9

[22] Balaj M, Roohi E, Akhlagi H and Myong R S 2014 Investigation of convective heat transfer through constant wall heat flux micro/nanochannels using DSMC. *Int. J. Heat Mass Transf.* 83: 633–638. doi:10.1016/j.ijheatmasstransfer.2013.12.053

[23] Balaj M, Roohi E and Akhlaghi H 2015 Effects of shear work on non-equilibrium heat transfer characteristics of rarefied gas flows through micro/nanochannels, *Int. J. Heat Mass Transf.* 83: 69–74. doi:10.1016/j.ijheatmasstransfer.2014.11.087

[24] Dongari N and Agrawal A 2012 Modeling of Navier–Stokes equations for high Knudsen number gas flows. *Int. J. Heat Mass Transf.* 55: 4352–4358. doi:10.1016/j.ijheatmasstransfer.2012.04.002

[25] Dongari N, Agrawal A and Agrawal A 2007 Analytical solution of gaseous slip in long microchannels. *Int. J. Heat Mass Transf.* 50: 3411–3421. doi:10.1016/j.ijheatmasstransfer.2007.01.048

[26] Cetin B 2013 Effect of thermal creep on heat transfer for a two-dimensional microchannel flow: an analytical approach. *J. Heat Transf.* 135: 101007-1-8. doi:10.1115/1.4024504

[27] Hettiarachchi H D M, Golubovic M, Worek W M and Minkowycz W J 2008 Three-dimensional laminar slip-flow and heat transfer in a rectangular microchannel with constant wall temperature. *Int. J. Heat Mass Transf.* 51: 5088–5096. doi:10.1016/j.ijheatmasstransfer.2008.02.049

[28] Sun W, Kakac S and A G Yazicioglu 2007 A numerical study of single-phase convective heat transfer in microtubes for slip flow. *Int. J. Therm. Sci*. 46: 1084–1094. doi:10.1016/j.ijthermalsci.2007.01.020

[29] Bao F and Lin J 2008 Burnett simulation of gas flow and heat transfer in micro Poiseuille flow. *Int. J. Heat Mass Transf.* 51: 4139–4144. doi:10.1016/j.ijheatmasstransfer.2007.12.009

[30] Demsis A, Verma B, Prabhu S V and Agrawal A 2010 Heat transfer coefficient of gas flowing in a circular tube under rarefied condition. *Int. J. Therm Sci.* 49: 1994–1999. doi:10.1016/j.ijthermalsci.2010.05.018

[31] Francisca J S and Tso C P 2009 Viscous dissipation effects on parallel plates with constant heat flux boundary conditions. *Int. Commun. Heat Mass Transf.* 36: 249–254. doi:10.1016/j.icheatmasstransfer.2008.11.003

[32] Zhu X 2003 Analysis of heat transfer between two unsymmetrically heated parallel plates with micro-spacing in the

slip flow regime. *Microscale Thermophys. Eng.* 6(4): 287–301. doi:10.1080/10893950290098311

[33] Shojaeian M, Yildiz M and Kosar A 2014 Heat transfer characteristics of plug flows with temperature-jump boundary conditions in parallel-plate channels and concentric annuli. *Int. J. Therm. Sci.* 84: 252–259. doi:10.1016/j.ijthermalsci.2014.05.014

[34] Kushwaha H M and Sahu S K 2015 The effects of viscous dissipation and rarefaction on parallel plates with constant heat flux boundary conditions. *Chem. Eng. Technol*. 38: 1–12. doi:10.1002/ceat.201400264

[35] Zhang T, Jia L, Yang L and Jaluria Y 2010 Effect of viscous heating on heat transfer performance in microchannel slip flow region. *Int. J. Heat Mass Transf.* 46: 4927–4934. doi:10.1016/j.ijheatmasstransfer.2010.05.055

[36] Sadeghi A and Saidi M H 2010 Viscous dissipation and rarefaction effects on laminar forced convection in microchannels. *J. Heat Transf.* 132: 072401-12. doi:10.1115/1.4001100

[37] Yazicioglu A G and Kakac S 2010 Convective heat transfer in microscale slip flow. In: Kakac S *et al* (eds.) *Microfluidics based microsystems: Fundamentals and applications.* 15. doi:10.1007/978-90-481-9029-4_2

[38] Liu H L, Shao X D and Jia J Y 2013 Effects of axial heat conduction and viscous dissipation on heat transfer in circular micro-channels. *Int. J. Therm. Sci.* 66: 34–41. doi:10.1016/j.ijthermalsci.2012.11.007